BRXL4-LAZY1 interaction at the plasma membrane controls Arabidopsis branch angle and gravitropism

Ximing Che (iD), Bessie L. Splitt, Magnus T. Eckholm (iD), Nathan D. Miller and Edgar P. Spalding* (iD)
Department of Botany, University of Wisconsin-Madison, Madison, WI 53706, USA

SUMMARY

Gravitropism guides growth to shape plant architecture above and below ground. Mutations in *LAZY1* impair stem gravitropism and cause less upright inflorescence branches (wider angles). The LAZY1 protein resides at the plasma membrane and in the nucleus. The plasma membrane pool is necessary and sufficient for setting branch angles. To investigate the molecular mechanism of LAZY1 function, we screened for LAZY1-interacting proteins in yeast. We identified BRXL4, a shoot-specific protein related to BREVIS RADIX. The BRXL4-LAZY1 interaction occurred at the plasma membrane in plant cells, and not detectably in the nucleus. Mutations in the C-terminus of LAZY1, but not other conserved regions, prevented the interaction. Opposite to *lazy1*, *brxl4* mutants displayed faster gravitropism and more upright branches. Overexpressing *BRXL4* produced strong *lazy1* phenotypes. The apparent negative regulation of LAZY1 function is consistent with BRXL4 reducing *LAZY1* expression or the amount of LAZY1 at the plasma membrane. Measurements indicated that both are true. *LAZY1* mRNA was three-fold more abundant in *brxl4* mutants and almost undetectable in *BRXL4* over-expressors. Plasma membrane LAZY1 was higher and nuclear LAZY1 lower in *brxl4* mutants compared with the wild type. To explain these results, we suggest that BRXL4 reduces the amount of LAZY1 at the plasma membrane where it functions in gravity signaling and promotes LAZY1 accumulation in the nucleus where it reduces *LAZY1* expression, possibly by suppressing its own transcription. This explanation of how BRXL4 negatively regulates LAZY1 suggests ways to modify shoot system architecture for practical purposes.

Keywords: BRXL4, gravitropism, LAZY1, shoot architecture, *Arabidopsis* genetics.

Linked article: This paper is the subject of a Research Highlight article. To view this Research Highlight article visit https://doi.org/10.1111/tpj.16076.

INTRODUCTION

Plants use gravitropism to align the growth of roots and shoots, and their branches, at angles that are genetically set yet subject to modification by environmental variables such as light, water, and nutrient gradients (Roychoudhry et al., 2017). Many molecular, cellular, and physiological events associated with gravitropism have been described (Morita, 2010; Su et al., 2017), but an end-to-end understanding of the complex and coordinated mechanism has not yet been achieved. Elucidating the mechanism would lead to a better understanding of how gravity-guided plant architecture affects resource acquisition and inter-plant competition below and above ground.

Gravitropism requires that an organ registers the direction of the gravity vector and then adjusts growth to align the organ with its gravitropic set-point angle (GSA). Cells containing dense amyloplasts that function as statoliths may register the direction of the gravity vector by determining which face of the cell the statoliths sediment

on (Su et al., 2017). Intracellular trafficking machinery then directs more auxin-transporting PIN proteins to the plasma membrane at this lowest face (Kleine-Vehn et al., 2010; Nakamura et al., 2019). Redirecting auxin produces a gradient that causes cells on opposite sides of the organ to elongate at different rates (Spalding, 2013). The resulting differential growth reorients the organ.

The present study concerns the role of a LAZY protein in the gravitropism mechanism. The first member of the *LAZY* gene family was identified by genetically mapping a mutation in rice responsible for wide tiller angles (Jones & Adair, 1938; Li et al., 2007; Yoshihara & Iino, 2007). The maize *lazy* mutant (van Overbeek, 1936) was subsequently shown to be a transposon-disrupted allele of a homologous gene (Dong et al., 2013; Howard et al., 2014). The Arabidopsis genome contains five genes that possess all five regions of conserved sequence (regions I–V) typical of *LAZY* genes (Yoshihara et al., 2013). A sixth Arabidopsis gene consists of only region V. Mutant analysis showed

that, of the five complete *LAZY* genes in Arabidopsis, *LAZY1* contributes the most to shoot system architecture (Yoshihara & Spalding, 2017). Branches emerge from the primary inflorescence stem of the wild type at an upright angle of approximately 45° but the branches of *lazy1* are almost horizontal (approximately 80°), due to impaired gravitropism rather than a stiffness defect (Yoshihara & Spalding, 2020).

If gravitropism consists of a detection phase, an auxin redistribution phase, and a growth control phase, LAZY proteins appear to act only in the first or to connect the first to the second (Jiao et al., 2021). Briefly, the evidence is that statoliths sediment normally in a *lazy1* mutant (Godbole et al., 1999; Taniguchi et al., 2017), a LAZY protein and an interacting protein redistribute in columella cells after gravistimulation (Godbole et al., 1999), an auxin gradient does not form following gravistimulation in various *lazy* mutants (Godbole et al., 1999; Overbeek, 1938; Yoshihara & Iino, 2007; Yoshihara & Spalding, 2017, 2020), but applying auxin to one side of a *lazy1* stem produces a normal differential growth response (Yoshihara & Spalding, 2020). The ability to establish an auxin gradient, but not the ability to respond to one, is impaired by *lazy* mutations.

In Arabidopsis, *LAZY1* is expressed at low levels throughout the shoot system (Yoshihara et al., 2013). Its protein is present at the plasma membrane and in the nucleus (Howard et al., 2014; Yoshihara et al., 2013). To obtain this result, it was necessary to insert green fluorescent protein (GFP) within a non-conserved region of LAZY1, because terminal fusions disrupted function. In addition, it was necessary to drive expression with a heat shock promoter in transgenic Arabidopsis seedlings, or the strong 35S promoter in *Nicotiana benthamiana* leaves to observe the fluorescent protein because of the low native expression level (Yoshihara et al., 2013; Yoshihara & Spalding, 2020). Experiments conducted in these systems showed that a mutation in region I that prevents LAZY1 from associating with the plasma membrane also prevents rescue of the *lazy1* branch angle defect (Yoshihara et al., 2013; Yoshihara & Spalding, 2020). Mutating a predicted nuclear localization signal (NLS) between regions III and IV prevents LAZY1 from accumulating in the nucleus but does not interfere with its GSA function (Yoshihara et al., 2013). *LAZY2* lacks an NLS and the protein is detected only at the plasma membrane. Expressing *LAZY2* under the control of the *LAZY1* promoter in a *lazy1* mutant completely rescued the branch angle phenotype (Yoshihara & Spalding, 2020). Thus, LAZY1 acts at the plasma membrane in a gravity-response process that sets branch angles. A study of rice LAZY1 reached the opposite conclusion, that nuclear OsLAZY1 was responsible for setting tiller angle (Li et al., 2019).

LAZY1 contains an EAR motif in the C-terminal region V. EAR motifs are associated with a mechanism for repressing transcription (Kagale & Rozwadowski, 2011; Yang et al., 2018). Nuclear localization and an EAR motif in a conserved and necessary region V indicate that LAZY1 regulates transcription. However, LAZY1 can rescue the branch angle phenotype of a *lazy1* mutant even when mutations in the NLS prevent the protein from accumulating in the nucleus (Yoshihara et al., 2013). These observations appear to contradict each other. The present study addresses this apparent contradiction while providing some molecular-level details about how LAZY1 and an interacting protein use gravity to orient stem structures.

RESULTS

LAZY1 interactor screen identifies BRXL4

Identifying a LAZY1 interacting protein may produce testable hypotheses about how LAZY1 functions in setting shoot architecture. Therefore, we screened an Arabidopsis cDNA library with the yeast two-hybrid (Y2H) method. Table S1 presents an annotated list of 16 putative LAZY1 interactors that we isolated more than once in the screen. One of the genes in this list, *BRX-like 4* (*BRXL4*; At5g20540) is the subject of the present study. The originally isolated clone was a gene fragment. Figure 1(a) shows that a full-length *BRXL4* cDNA produced a strong interaction with LAZY1 when presented as bait or prey.

BRXL4 physically interacts with LAZY1 at the plasma membrane *in planta*

Like LAZY1, BRXL4 is located at the plasma membrane and nucleus when transiently expressed in *N. benthamiana* leaves (Figure 1b,c), but bimolecular fluorescence complementation (BiFC) mediated by BRXL4-LAZY1 interaction is apparently restricted to the plasma membrane (Figure 1d, e). The BiFC result was the same regardless of which protein carried the nYFP or cYFP half of the yellow fluorescent reporter (Figure 1d,e). These results confirm that the BRXL4-LAZY1 interaction in yeast also occurs in plant cells, and they indicate that the interaction is conditional. The plasma membrane and nucleus may differ with respect to factors that affect the conformation or accessibility of a LAZY1 or BRXL4 binding site. Neither nYFP-LAZY1 nor nYFP-BRXL4 interacts with free cYFP, a standard control test (Figure S1).

BRXL4 is one of five Arabidopsis genes in a family founded by the *BREVIS RADIX* (*BRX*) gene (Briggs et al., 2006; Mouchel et al., 2004). Like the *LAZY* family, *BRXL* genes occur only in plants. BRXL proteins have no known or predicted enzymatic function, but they all have two large BRX domains (Figure 2a) that have been shown to facilitate protein–protein interactions (Briggs et al., 2006) and to associate with membranes (Koh et al., 2021). Proteins may associate with membranes via basic and hydrophobic (BH) domains (Barbosa et al., 2016). A
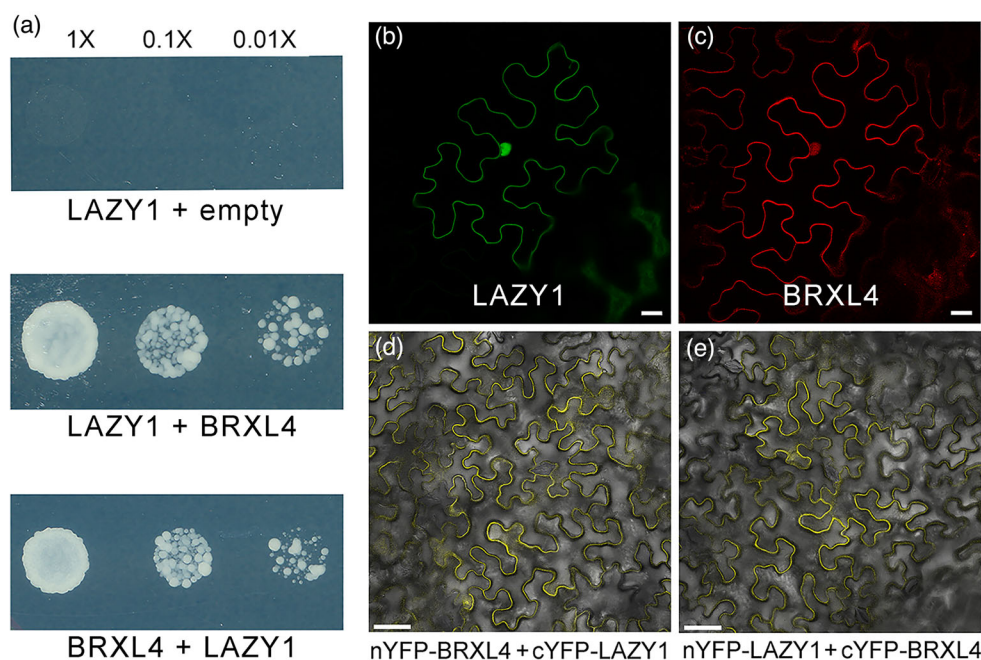
Figure 1. BRXL4 physically interacts with LAZY1 in yeast and in plant cells.

(a) A dilution series of yeast grown for 3 days on selective media also containing 20 mM 3-AT, an inhibitor of autoactivation. The displayed result is representative of five independent trials. Cells containing LAZY1 presented as bait with an empty prey vector (control) did not grow. Cells with LAZY1 bait and BRXL4 prey grew, indicating interaction, as did cells with BRXL4 bait and LAZY1 prey.

(b) Subcellular localization of LAZY1 tagged with GFP and (c) BRXL4 tagged with RFP co-expressed in *Nicotiana benthamiana* leaf epidermal cells. Both proteins appear at the plasma membrane and in the nucleus. Scale bar = 20 μm.

(d) Bimolecular fluorescence complementation assay in *N. benthamiana* leaf epidermal cells. LAZY1 interacts with BRXL4 to join functionally the amino-terminal half of YFP (nYFP) to the carboxy terminal half (cYFP), at the plasma membrane but not the nucleus, indicated by the yellow fluorescence signal.

(e) The interaction was also evident when the molecules were presented in the other the possible configuration. Scale bar = 50 μm.

software program (Brzeska et al., 2010; https://hpcwebapps.cit.nih.gov/bhsearch/) that successfully predicted membrane-associating BH domains in Arabidopsis proteins (Reuter et al., 2021) predicted two BH domains in BRXL4, one in each of the BRX domains (Figure 2a). The same analysis of the LAZY1 sequence predicted a BH domain in region I (Figure 2b) that included the residues previously found to be necessary for localizing LAZY1 to the plasma membrane (Yoshihara et al., 2013). However, this BH domain cannot fully explain LAZY1 membrane association because region I alone does not target GFP to the plasma membrane (Yoshihara & Spalding, 2020). A second predicted BH domain within the NLS region and a third within region IV (Figure 2b) may augment LAZY1 membrane association. Figure S3 shows the full BH score profiles for the BRXL4 and LAZY1 sequences.

Previous LAZY1 structure–function studies identified conserved amino acids in region I, II, and V that disrupt LAZY1 GSA function when changed to alanine (Yoshihara & Spalding, 2020). Figure 2(b) shows that the disabling mutations in region I, which disrupt association with the plasma membrane, or region II did not affect the LAZY1-BRXL4 interaction, while the mutations in each of the three different locations in region V greatly diminished the LAZY1-BRXL4 interaction. These results are evidence of a functionally relevant interaction between BRXL4 and region V of LAZY1. A previous study used rice LAZY1 (OsLAZY1) as a Y2H bait and identified OsBRXL4 as an interactor (Li et al., 2019). Deleting the BRX domain of OsBRXL4 prevented the interaction.

BRXL4 negatively regulates branch angle in Arabidopsis

If the physical interaction between BRXL4 and LAZY1 at the plasma membrane is functionally important, then a *brxl4* knockout mutant should display a branch angle phenotype. Two different lines with T-DNA inserted in the fifth exon of *BRXL4* were obtained. Both *brxl4-1* and *brxl4-2* mutants displayed an upright inflorescence architecture with branch angles being approximately 39° compared with approximately 48° for wild type (Figure 3a–c,h). This phenotype is opposite to *lazy1*, which produces branch angles that are approximately 30° wider than wild type, approximately horizontal (Figure 3d,h). If *BRXL4* is a negative regulator of branch angle as the mutant phenotypes indicate, a *BRXL4* overexpressor should show wider branch angles and an inflorescence architecture like that of *lazy1*. We generated a *BRXL4* overexpressor by transforming a wild-type plant with a copy of *BRXL4* under its native
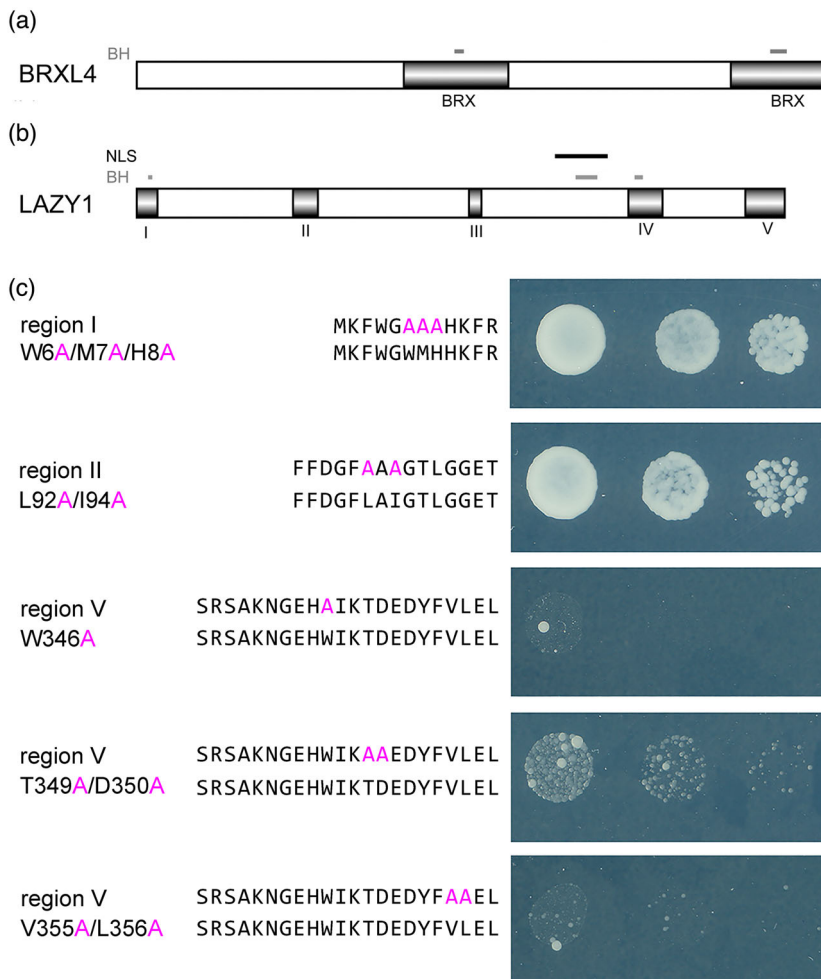
(a)

BRXL4

(b)

LAZY1

(c)

region I W6A/M7A/H8A	MKFWGAAAHKFR MKFWGWMHHKFR	
region II L92A/I94A	FFDGFAAAGTLGGET FFDGFLAIGTLGGET	
region V W346A	SRSAKNGEHAIKTDEDYFVLEL SRSAKNGEHWIKTDEDYFVLEL	
region V T349A/D350A	SRSAKNGEHWIKAAEDYFVLEL SRSAKNGEHWIKTDEDYFVLEL	
region V V355A/L356A	SRSAKNGEHWIKTDEDYFAAEL SRSAKNGEHWIKTDEDYFVLEL	

Figure 2. Structural features of BRXL4 and LAZY1 and their relevance to physical interaction.

(a) BRXL4 is a 384 amino acid protein containing two BRX domains. A BH domain is predicted within each BRX domain.

(b) LAZY1 is a 358 amino acid protein with five regions of substantial sequence conservation (I–V), a nuclear localization signal (NLS) and three predicted BH domains. The BH domain in region I contains the residues known to be required for associating LAZY1 with the plasma membrane. Another BH domain lies within the NLS.

(c) Highly conserved residues in LAZY1 were replaced with alanine. Mutations in regions I and II did not affect BRXL4-LAZY1 interaction in a yeast two-hybrid assay performed as in Figure 1, but three different alterations in region V greatly diminished the interaction.

promoter (*proBRXL4*), and another version based on the strong, constitutive 35S promoter (*pro35S*). The *proBRXL4* plant displayed horizontal (approximately 90°) *lazy1*-like branch angles (Figure 3e,h). The *pro35S* line displayed even greater (approximately 120°) branch angles (Figure 3f,h). Figure S2 shows additional examples of these shoot architecture phenotypes.

The results in Figure 3 show that *brxl4* and *lazy1* have opposite phenotypes, which presents an opportunity to determine which phenotype prevails in a double mutant, which can establish the order of action between the interacting proteins. The *brxl4 lazy1* double mutant exhibited *lazy1*-like wide branch angles rather than more upright, *brxl4*-like branch angles (Figure 3g,h). If modeled as a linear signaling pathway, BRXL4 therefore acts negatively upstream of LAZY1.

The expression patterns of *BRXL4* and *LAZY1* would be expected to overlap in the organs displaying altered GSA if the protein interaction is mechanistically relevant. We expressed a *proBRXL4:GFP-NLS* reporter gene in a wild-type plant. GFP signals indicative of BRXL4 promoter activity were evident in mature shoots in the node region including newly emerging axillary buds (Figure 4a–c). In etiolated seedlings, expression was evident in the hypocotyl (Figure 4d). Expression was noted at the base of flowers and siliques (Figure 4e,f). These sites of expression are very similar to those reported for *LAZY1* (Hollender et al., 2020; Yoshihara et al., 2013), supporting the conclusion that BRXL4 and LAZY1 proteins act together to determine branch angle.

BRXL4 negatively regulates gravitropism

The wide branch angle of *lazy1* is associated with defective gravitropism (Yoshihara et al., 2013). If *BRXL4* negatively regulates *LAZY1* then *brxl4* mutants should respond more strongly in a gravitropism assay. We tested this hypothesis using excised inflorescence stems as described previously (Yoshihara & Spalding, 2020) except in this case we developed custom software to automate the image analysis. The assay demonstrated hypergravitropism in both *brxl4* alleles, impaired gravitropism in the *proBRXL4* overexpressing line, and almost no gravitropism in the *pro35S*

Figure 3. Shoot architecture phenotypes associated with *BRXL4* mutation and overexpression.

(a) Wild type, (b) *brxl4-1*, (c) *brxl4-2*, (d) *lazy1*, (e) wild-type plant transformed with *BRXL4* controlled by the *BRXL4* promoter, (f) wild-type plant transformed with *BRXL4* controlled by the strong *35S* promoter, and (g) *brxl4 lazy1* double mutant. A thin wire connected to the shoot apex was gently lifted with a micromanipulator to straighten the main inflorescence stem so branch angles could be clearly seen in each photographs. (h) Angle of the first-formed branch for the genotypes shown in (a–g). The *brxl4* alleles have a significantly smaller angle than wild type, *P < 0.01 as determined by Student's *t*-test. Box size denotes the standard error of the mean.
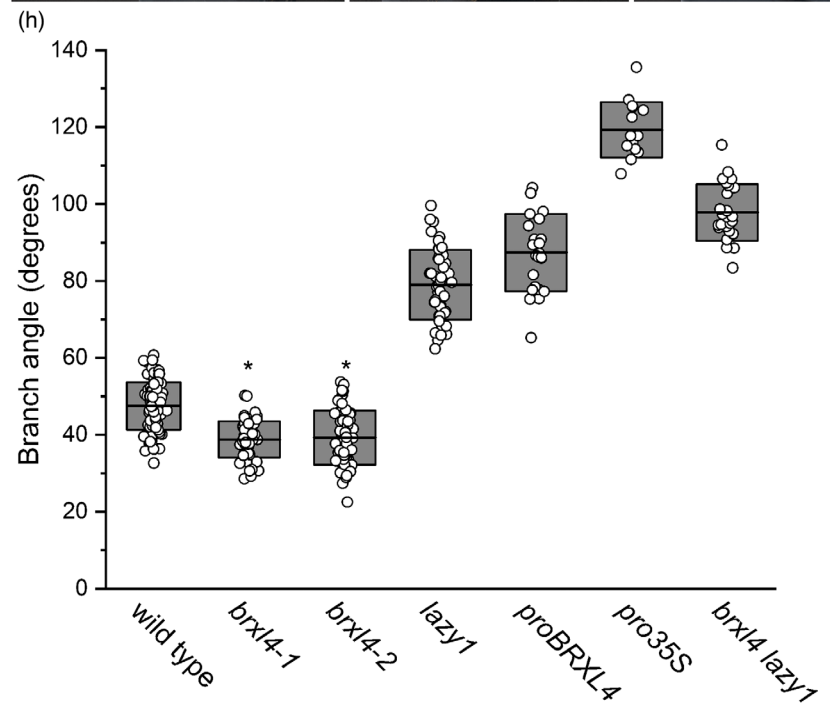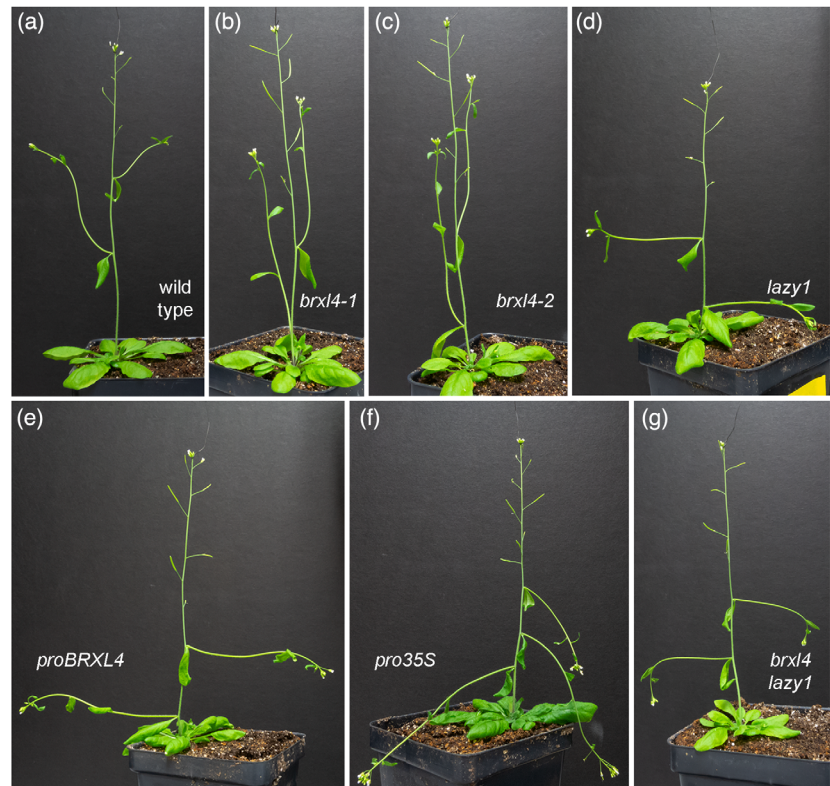
line (Figure 5a,b; Movie S1). One hour after being placed horizontal, *brxl4* inflorescence stems achieved an angle of 90°, the wild type had reached 45°, and *proBRXL4* barely exceeded 10° (Figure 5a,b). The *pro35S* line had not yet begun to respond 1 h after 90° rotation.

Gravitropism of etiolated hypocotyls was also tested. Images were automatically collected in complete darkness using infrared illumination. Like the inflorescence stem result, both *brxl4-1* and *brxl4-2* displayed faster and greater gravitropism than wild type (Movie S2), achieving
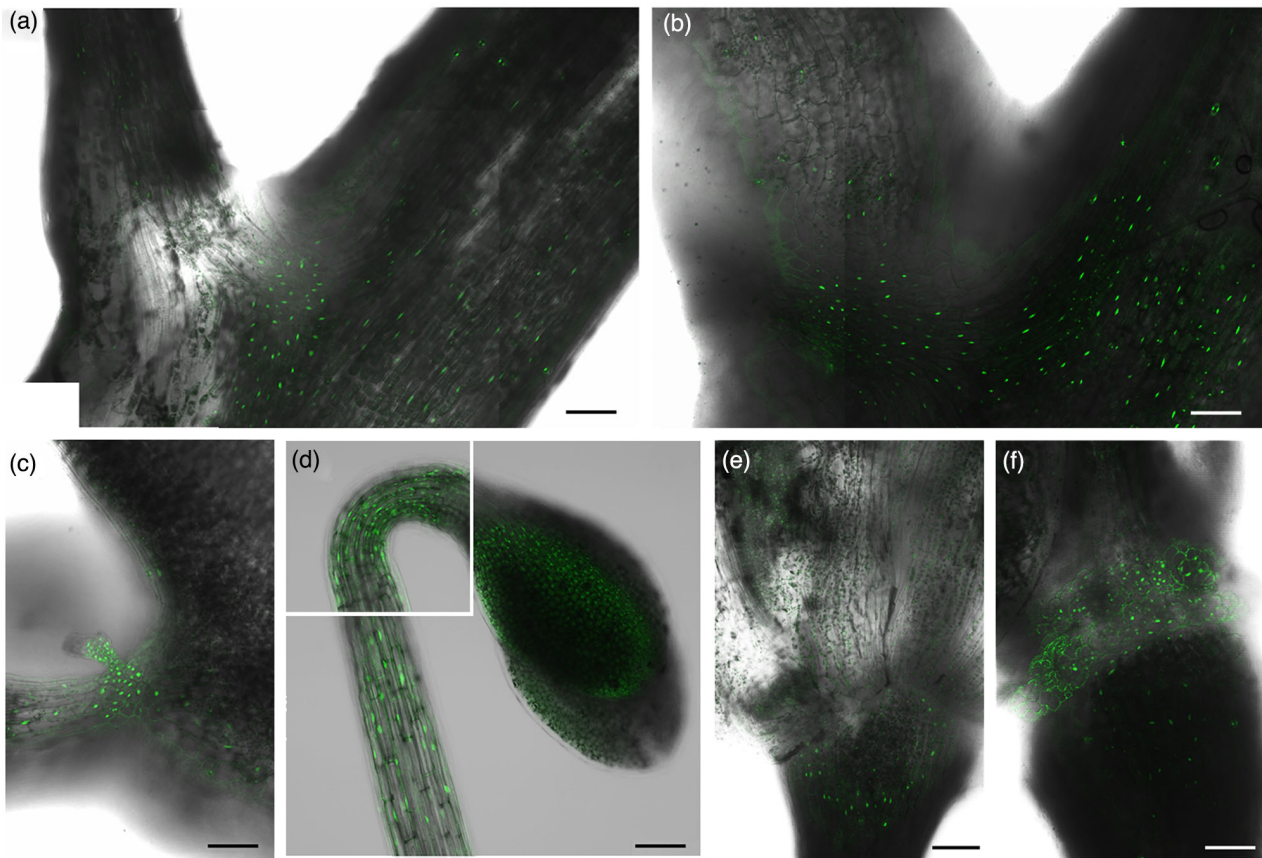
Figure 4. *BRXL4* expression pattern visualized by expressing a nuclear-localized version of GFP controlled by the *BRXL4* promoter.
Expression is evident in the nodes of the inflorescence stem and branch bases (a,b), in axillary buds (c), throughout etiolated hypocotyls (d), at the base of flowers (e), and siliques (f). Some pictures were prepared by overlapping separate frames. Scale bar = 200 μm except (a), which is 400 μm.

approximately 65° at the end of 6 h, while the wild type more slowly reached a final angle of 45° (Figure 5c,d). Hypocotyl gravitropism in *proBRXL4* was greatly diminished, and the *pro35S* line was essentially agravitropic (Figure 5c,d). We conclude that the steeper branch angle phenotype of *brxl4* mutants (Figure 3) is a consequence of enhanced gravitropism (Figure 5) due to disabled negative regulation of *LAZY1*.

BRXL4 negatively regulates *LAZY1* expression

A negative effect of *BRXL4* on *LAZY1* expression could explain the mutant phenotypes. Consistent with this possibility, Figure 6(a) shows that the two *brxl4* alleles, which expressed little or only trace amounts of *BRXL4* mRNA (Figure 6b), expressed approximately three-fold more *LAZY1* mRNA, compared with the wild type, in inflorescence stems and etiolated hypocotyls. Furthermore, overexpressing *BRXL4* reduced *LAZY1* mRNA. The *proBRXL4* plant, which overexpressed *BRXL4* by 3.5-fold (Figure 6b) displayed approximately 50% of the wild-type level of *LAZY1* mRNA in inflorescence stems (Figure 6a). Overexpressing *BRXL4* approximately 80-fold in hypocotyls and

40-fold in inflorescence stems with the 35S promoter (Figure 6b) reduced *LAZY1* mRNA to undetectable levels (Figure 6a). These results demonstrate a dosage-dependent negative effect of *BRXL4* on *LAZY1* expression.

BRXL4 affects LAZY1 subcellular distribution

Figure 7(a,b) shows representative confocal microscope images of LAZY1-GFP subcellular localization in *lazy1* and *brxl4* hypocotyls after expression was induced by a temperature treatment (heat shock) as previously described (Yoshihara et al., 2013; Yoshihara & Spalding, 2020). In *brxl4* hypocotyls, we consistently observed stronger LAZY1-GFP fluorescence at the plasma membrane and weaker signal in the nucleus compared with the "wild-type" situation (LAZY1-GFP expressed in a *lazy1* background). To quantify these differences objectively, we developed custom image analysis software. Figure 7(c) shows an example of the automated plasma membrane sampling method. The results show that *brxl4* accumulated significantly more LAZY1 at the plasma membrane and less in the nucleus (Figure 7d). Thus, BRXL4 affects the subcellular distribution of LAZY1 in a way that is
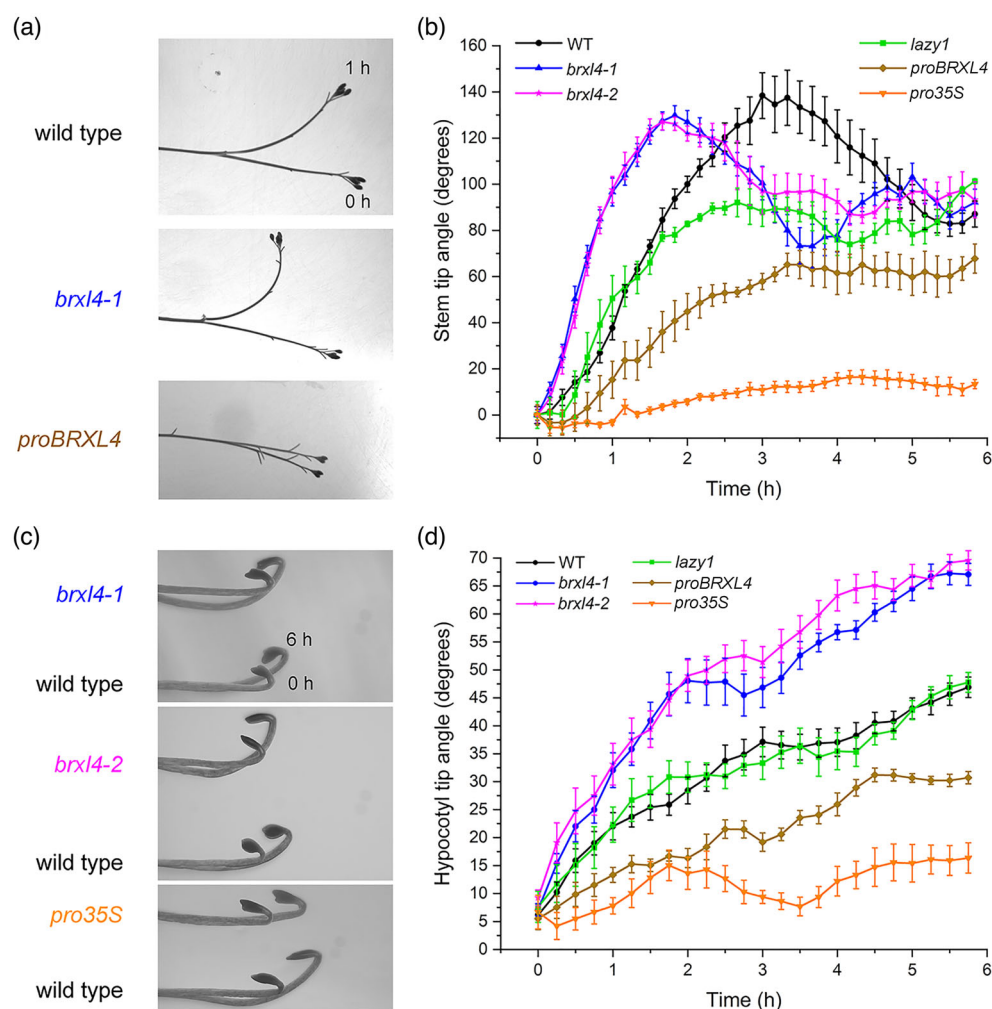
Figure 5. Gravitropism phenotypes of *brxl4* mutants and *BRXL4* overexpressors compared with *lazy1* and double mutants.
(a) Inflorescence gravitropism examples. Excised primary inflorescence stems are shown when rotated horizontally and 1 h later. Hypergravitropism of *brxl4* and weak gravitropism of *proBRXL4* are evident.
(b) Time course of inflorescence gravitropism measured by automated image analysis shows faster, hypergravitropism of two *brxl4* alleles and suppressed gravitropism in plants overexpressing *BRXL4*. Error bars denote standard error of the mean. WT, wild type.
(c) Etiolated hypocotyl gravitropism examples. Intact seedlings are shown when rotated horizontally and 6 h later.
(d) Time course analysis shows faster, hypergravitropism of two *brxl4* alleles and suppressed gravitropism in plants overexpressing *BRXL4*. Error bars denote standard error of the mean.

consistent with its hypergravitropic phenotypes, assuming that the plasma membrane pool mediates gravity signaling. Based on the effect of the *brxl4* mutation, we predicted that overexpressing *BRXL4* would increase the amount of LAZY1 in the nucleus. This prediction was observed, but so were some unpredicted effects. Figure S4 shows that LAZY1-GFP in *pro35S* lines formed bright spots in the nucleus and accumulated in the cytoplasm. The cytoplasmic signal was difficult to distinguish from the plasma membrane signal in many cases so the images in Figure S4 were not processed with the automated quantification software. The large amount of LAZY1 in the cytoplasm of *BRXL4* OE lines may reflect LAZY1 backed up in the process of being transported to the nucleus and/or the result

of a mechanism for exporting excess LAZY1 protein from the nucleus.

DISCUSSION

The small family of Arabidopsis *BRXL* genes founded by *BREVIS RADIX* is defined primarily by two similar sequences of 55 amino acids (BRX domains) separated by a variable sequence of at least 100 amino acids (Briggs et al., 2006). BRX domains occur in proteins outside of this family, and they can function in protein–protein interactions. Most relevant to the present study, a BRX domain in the RLD protein was recently shown to interact with region V of LAZY4 (Furutani et al., 2020). Deleting entire BRX domains from a rice BRXL protein (OsBRXL4) prevented its
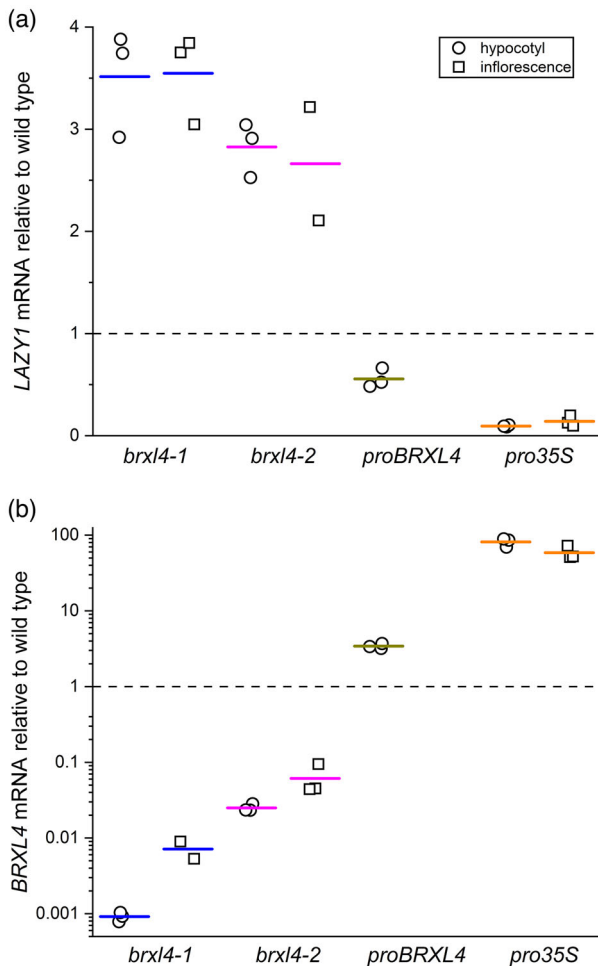
Figure 6. *LAZY1* expression is inversely related to *BRXL4* expression.
(a) *LAZY1* mRNA level is approximately three-fold higher in *brxl4* than in the wild type, in hypocotyls and inflorescence stems. Expressing *BRXL4* with its native promoter (*proBRXL4*) in the wild type reduced *LAZY1* expression by approximately 50%, and to nearly undetectable levels when the 35S promoter (*pro35S*) controlled expression. *LAZY1* mRNA was not measured in *proBRXL4* inflorescence stems.
(b) No or very low *BRXL4* expression was measured in the *brxl4* alleles, while *proBRXL4* increased *BRXL4* mRNA approximately three-fold, and the *pro35S:BRXL4* construct increased *BRXL4* mRNA approximately 80-fold in hypocotyls. Note the logarithmic scale of the y-axis. Each symbol represents an independent experiment, i.e., separate biological replicate normalize to the average wild-type value determined for that tissue (hypocotyl or inflorescence). The three measurements of wild-type BRXL4 and LAZY1 levels were very consistent in both tissue types. The SD of the wild-type measurements of *BRXL4* and *LAZY1* mRNA in hypocotyls and inflorescence stems ranged from 9% to 17% of the mean, insignificant relative to the genotype effects.

interaction with OsLAZY1 (Li et al., 2019), consistent with the effects of site-directed mutations within region V on the Arabidopsis BRXL4-LAZY1 interaction (Figure 2b). BRX domains also associate proteins with membranes. An engineered fluorescent protein consisting only of two BRX domains and the intervening linker localized to the plasma membrane in root cells (Koh et al., 2021). Predicted

membrane-associating BH domains within the BRX domains of BRXL4 (Figure 1b) may explain the plasma membrane localization of BRXL4.

In Figure 8 we illustrate how BRXL4 and LAZY1 may work together to affect gravitropism and branch GSA. The model is consistent with the experimental results in Figures 1–7 but its components should be viewed as hypotheses to be tested. We propose that the BH domains of LAZY1 interact with the plasma membrane, where the protein performs its GSA signaling function in a wild-type plant (Figure 8a). We previously showed that mutating the BH domain in region I prevents LAZY1 from localizing to the plasma membrane and makes it non-functional with respect to setting GSA (Yoshihara & Spalding, 2020), so this suggestion has some basis in fact. A BH domain between regions III and IV lies within the LAZY1 NLS (Figure 2b). If this BH domain is also a membrane association site, the NLS may be blocked from binding to importin α, a principal component in the mechanism that brings NLS-containing proteins to the nucleus (Chang et al., 2012; Smith & Raikhel, 1999). Membrane-associated LAZY1 may be a poor substrate for the nuclear import mechanism until interaction with BRXL4 makes the NLS in LAZY1 more accessible (Figure 8a). BRXL4-dependent LAZY1 redistribution would explain why *brxl4* cells have more LAZY1 at the plasma membrane and less in the nucleus than wild type (Figure 7). Extra LAZY1 at the membrane performing a gravity signaling function (Figure 8b) is consistent with more upright branches and hypergravitropism in *brxl4* (Figures 3 and 5). Less LAZY1 in a *brxl4* nucleus (Figure 7d) yet approximately three-fold more *LAZY1* mRNA (Figure 6a) is consistent with nuclear LAZY1 inhibiting *LAZY1* expression. The present results do not explain how LAZY1 reduces *LAZY1* mRNA levels. We speculate that the mechanism involves interaction between the EAR motif in LAZY1 and a direct or indirect modifier of *LAZY1* transcription. LAZY1 does not contain a recognizable DNA-binding domain so we believe interaction with a promoter sequence is unlikely. In addition, EAR motifs typically affect expression by binding to transcriptional regulators such as TPL (Kagale & Rozwadowski, 2011). A transcriptional regulator in the nucleus with a high affinity for LAZY1 could replace BRXL4 as a binding partner, potentially explaining the lack of detectable BRXL4-LAZY1 interaction in the nucleus (Figure 1d,e). Unfortunately, no candidates for this hypothetical regulator were discovered in the Y2H screen (Table S1). According to this model, and consistent with observations, overexpressing *BRXL4* produces essentially agravitropic shoots (Figures 3 and 5) by increasing the nuclear LAZY1 pool (Figures 7 and 8c; Figure S4).

Future experiments may show that the mechanism is much more complicated than BRXL4 mediating the balance between membrane-associated and nuclear LAZY1.
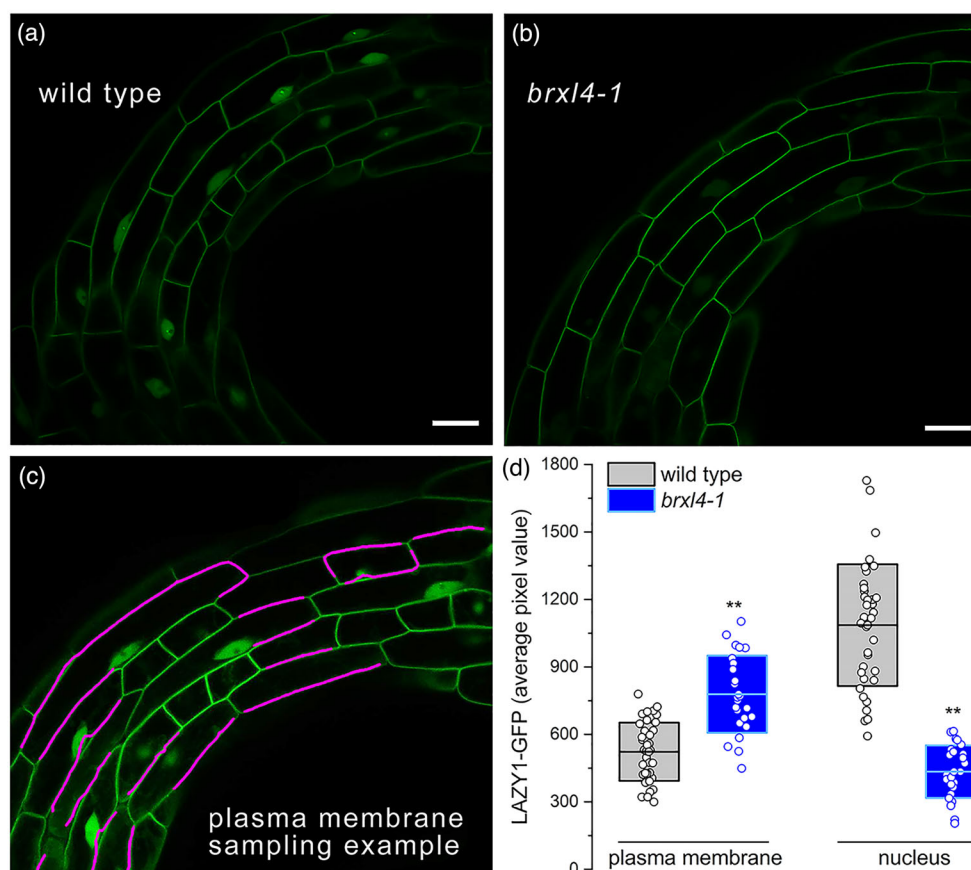
Figure 7. BRXL4 affects LAZY1 subcellular distribution.

(a) LAZY1-GFP was present at the plasma membrane and in the nucleus when expressed in a *lazy1* mutant (wild-type context) controlled by a heat-shock promoter to produce measurable signals.

(b) LAZY1-GFP was primarily at the plasma membrane and secondarily in the nucleus when expressed in a *brxl4-1* mutant. Scale bar = 20 μm.

(c) Magenta lines show the regions of an example image that the custom analysis method automatically sampled to determine the GFP level at the plasma membrane.

(d) The average GFP channel value for plasma membrane or nuclear pixels in the indicated genotypes. Each symbol represents the average pixel value sampled from the plasma membranes or nuclei in one image, and each image represents a separate hypocotyl. Box size denotes standard error of the mean. **brxl4* values are significantly different from the wild type at $P = 0.01$ as determined by a Student's *t*-test.

Studies of the related BRX protein conclude that auxin induces BRX movement from the plasma membrane to the nucleus in roots (Koh et al., 2021; Scacchi et al., 2009) where it influences the differentiation of root protophloem cells (Marhava et al., 2018, 2020). If auxin similarly affects BRXL4 movement to the nucleus, the auxin gradients that form downstream of LAZY1 after gravistimulation may result in a gradient of BRXL4-LAZY1 interaction across a stem during gravitropism. If LAZY1 is required to form gravity-induced auxin gradients and BRXL4 negatively regulates LAZY1 function via interaction, and if auxin affects BRXL4 subcellular localization, the potential for complicated feedback regulation is great.

The model in Figure 8 differs significantly from the conclusions of a previous study of rice LAZY1 (OsLAZY1), even though some of the results are consistent. Li et al. (2019) screened for OsLAZY1 interactors and found

OsBRXL4. Their *OsBRXL4* overexpressing lines appeared *lazy1*-like (wider tiller angle) and RNAi knockdown lines displayed narrower tiller angles, consistent with the Arabidopsis phenotype data in Figure 3. However, Li et al. (2019) concluded that the rice BRXL4 protein reduces, rather than promotes, nuclear localization of OsLAZY1 and they concluded that nuclear OsLAZY1 mediates gravity signaling. A step in the rice mechanism may be reversed compared with Arabidopsis. Either LAZY1 or BRXL4 may function oppositely in rice. However, the phenotypes of the Arabidopsis and rice *lazy1* mutants are similar (wider branch GSA). A phylogenetic analysis showed that monocot and dicot *BRXL* genes cluster separately, which may indicate major functional differences (Beuchat et al., 2010). However, rice *BRXL* genes could rescue the root growth phenotype of the Arabidopsis *brx* mutant, indicating they have some degree of common function (Beuchat
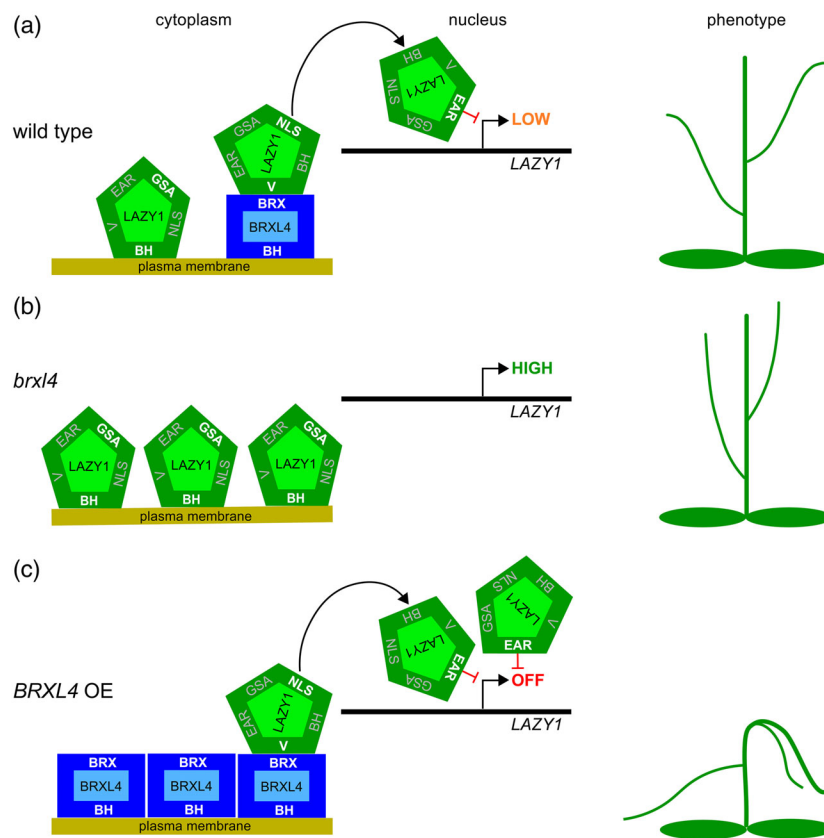
Figure 8. BRXL4 may negatively regulate LAZY1 by shifting it from the plasma membrane, where it functions in gravity signaling, to the nucleus, where it may suppress its own expression.

(a) According to this model, the basic–hydrophobic (BH) domains of LAZY1 interact with the plasma membrane. LAZY1-mediated gravity signaling sets the gravity setpoint angle (GSA) of branches. The transcription-repressing EAR domain, the nuclear localization sequence (NLS), and the BRX-interacting region V (V) are inoperative in this situation and are therefore shown in gray. BRXL4 associates with the plasma membrane via the BH domain and with region V of LAZY1 via the BRX domain, which enables the NLS to promote transport of the LAZY1 to the nucleus where the EAR domain suppresses expression of *LAZY1*.

(b) In a *brxl4* mutant, LAZY1 remains at the plasma membrane with its GSA function active and its NLS function suppressed. The resulting *LAZY1* overexpression produces hyperactive gravitropism and steeper branch angles.

(c) *BRXL4* overexpression shifts more LAZY1 from the plasma membrane to the nucleus where its EAR domain suppresses its own expression, resulting in weak gravitropism and wide branch angles.

et al., 2010). Instead of a fundamental difference in the BRXL4-LAZY1 GSA mechanism (Wang et al., 2021), differences in experimental methodologies may explain the opposite conclusions.

In the present study (Figure 1b–e) and in previous studies (Yoshihara et al., 2013; Yoshihara & Spalding, 2020), we found LAZY1 residing at the plasma membrane and/or nucleus (depending on the experiment) in *Nicotiana benthamiana* leaves and Arabidopsis hypocotyls, with typically no signal in the cytoplasm. Our GFP-tagged LAZY1 typically rescues the branch angle phenotype of *lazy1* mutants, indicating the tagged protein is functional. To obtain this functional GFP-tagged LAZY1, we had to insert the GFP within the gene body, between Lys308 and Ala309 (Yoshihara et al., 2013). Terminal tags did not function as determined by mutant rescuing tests. Li et al. (2019) fused mCherry to the C-terminus of OsLAZY1 and did not demonstrate that the tagged protein could

rescue the rice *lazy1* mutant. When expressed in rice protoplasts, the OsLAZY1-mCherry reporter was evident in the cytoplasm and nucleus, and possibly not at the plasma membrane. They base their conclusion that OsBRXL4 acts to reduce OsLAZY1 nuclear localization largely on a reduction in the visually scored presence or absence of OsLAZY1-mCherry in the nucleus of protoplasts transfected with different amounts of *OsBRXL4* plasmid (Li et al., 2019). We used a different assay. We quantified the change in LAZY1 abundance at the plasma membrane and nucleus caused by a *brxl4* mutation (Figure 7d).

Regarding architectural phenotypes, Yoshihara et al. measured branch angles in more than 100 transgenic plants (individual T1 plants) transformed with NLS-mutated *LAZY1*, and a similar number of control plants transformed with wild-type *LAZY1*, to demonstrate that rescue of the *lazy1* phenotype did not require LAZY1 in the nucleus (Yoshihara et al., 2013; Yoshihara &

Spalding, 2020). Statistically analyzing the distribution of the branch angles showed that even the wild-type *LAZY1* gene would not always rescue the phenotype, possibly because of insertion position effects on transgene expression (Yoshihara & Spalding, 2020). Pictures showing wide tiller angles in two transgenic lines support the conclusion that NLS-mutated OsLAZY1 cannot rescue the tiller angle phenotype (Li et al., 2019). A quantitative analysis of many more lines may show that an NLS-mutated *OsLAZY1* usually can rescue the tiller angle phenotype as found in Arabidopsis.

If opposite conclusions about the role of BRXL4 and the functions of nuclear LAZY1 are better explained by differences in experimental details than by opposite mechanisms operating in Arabidopsis and rice (Wang et al., 2021), then the results reported here may establish a general framework for setting branch angles in all terrestrial plants. Downstream of gravity vector detection and upstream of auxin redistribution, the physical and molecular-genetic interplay between BRXL4 and LAZY1 may constitute a middle stage in a process that determines land plant shoot architecture. Other proteins surely play roles during this stage. Future work should investigate if the model in Figure 8 can accommodate a role for *TILLER ANGLE CONTROL 1* (*TAC1*), a gene that belongs to the IGT superfamily, of which the *LAZYs* are a subgroup (Waite & Dardick, 2021). A *tac1* mutant displays more erect branches, much like *brxl4*, and functions to integrate effects of photosynthesis on shoot architecture (Waite & Dardick, 2018). Like *brxl4*, *tac1* is epistatic to *lazy1* (Hollender et al., 2020).

In addition to positioning leaves in ways that determine canopy photosynthesis, shoot architecture can influence reproductive success. Wender et al. (2005) reported that branch angle is one of the genetically determined variables that explains Arabidopsis seed dispersion patterns, particularly when plant density is significant. Thus, the BRXL4-LAZY1 stage of the GSA setting mechanism may affect ecological competitiveness. Selection may have acted on this stage of the process to produce the great variety of branch angles observable in nature more so than the vector detection or differential growth stages. The BRXL4-LAZY1 stage may be where natural selection mediates the tradeoffs between energy harvesting, density tolerance, reproduction strategies, and various contingencies. Some evidence supports this suggestion. A recent study of tiller angle in the barnyard grass weed (*Echinochloa crus-galli*) indicated that selection has acted on this stage of the GSA-setting mechanism (Ye et al., 2019). A rice-like form of the weed (narrow tiller angles) is found in Chinese rice paddies, apparently because farmers notice and remove individuals with wider tiller angles that are typical of non-paddy environments. Genome sequencing identified *LAZY1* as one of the genes responsible for this

human-assisted, inadvertent selection of a crop mimicking phenotype (Ye et al., 2019). Intentional selection of crop species, including trees has produced a great variety of branch GSAs, with more upright branches often desired because they allow higher density plantings (Dardick et al., 2017; Waite & Dardick, 2021). Thus, the results presented here may help to produce a better understanding of shoot architecture evolution and show how shoot architecture could be engineered for practical purposes.

EXPERIMENTAL PROCEDURES

Yeast two-hybrid library screen and targeted validation assays

A GAL4-based yeast two-hybrid system was used to screen for plant protein–protein interactions in yeast. A library of Arabidopsis shoot apex-derived cDNA in pEXP-AD502 vectors was kindly provided by Scott Michaels (Indiana University, Bloomington, IN, USA). AH109 yeast cells containing pDEST32-LAZY1 were transformed with the cDNA library, and then spread on synthetic dropout media lacking Trp, Leu, and His (SDIII), and supplemented with 20 mM 3-amino-1, 2, 4-triazol to suppress autoactivation. After incubating the plates at 30°C for 4 days, yeast plasmids were extracted from many vigorously growing colonies using Zymoprep Yeast Plasmid Miniprep (www.zymoresearch.com). The cDNA portion of the pEXP-AD502 plasmid was amplified by polymerase chain reaction (PCR), sequenced, and subjected to BLAST analysis to identify putative LAZY1 interactors.

For targeted Y2H assays, AH109 yeast cells were co-transformed with the bait (pDEST32) and prey (pDEST22) plasmids containing the indicated inserts, then spread on media lacking Trp and Leu (SDII). After growing for 3 days at 30°C, five individual colonies were picked and transferred to SDII liquid media. After growth overnight, the cultures were adjusted to an OD_{600} of 1.0 by addition of liquid medium and then diluted 10-fold and 100-fold to produce a series of samples that were spotted on plates containing SDIII + 20 mM 3-amino-1,2,4-triazol media. Some targets were point mutations of *LAZY1* created with the Phusion Site-Directed Mutagenesis Kit (www.thermofisher.com).

Subcellular localization and BiFC in *Nicotiana benthamiana* leaves

RFP was fused to the N-terminus of BRXL4, for the purpose of determining subcellular localization, by cloning the *BRXL4* cDNA into the pUBN-RFP-DEST vector. Mouchel et al. (2004) demonstrated that GFP attached to the N-terminus of BRX did not interfere with its function. To localize LAZY1, eGFP was inserted within a non-conserved region of the coding sequence as Yoshihara et al. (2013) previously described and placed under the control of the 35S promoter to create the *35S:LAZY1-GFP* construct. For the BiFC assay, the *BRXL4* and *LAZY1* cDNA sequences were cloned into the pDOE8 BiFC vector (Gookin & Assmann, 2014) using the SanDI cutting site in MCS3 and the *PacI* cutting site in MCS1.

Leaves of *N. benthamiana* were infiltrated with the GV3101 strain of *Agrobacterium tumefaciens* containing the completed constructs to express transiently the resulting BRXL4 and/or LAZY1 fusion proteins. a Zeiss 710 laser-scanning confocal microscope was used to collect mVenus fluorescence (520–585 nm) and *eGFP* fluorescence (500–560 nm) excited by a 488 nm laser, and *mRFP* fluorescence (570–640 nm) excited by a 561 nm argon laser 2 days after infiltration.

Arabidopsis mutants and transgenic plants

The Columbia ecotype (Col-0) of *Arabidopsis thaliana* was the wild type used in this study. The *lazy1* T-DNA insertion mutant was previously described by Yoshihara et al. (2013). The Arabidopsis Biological Resources Center supplied the *brxl4-1* (SALK_147349c) and *brxl4-2* (SALK_022411c) T-DNA insertion mutants. The gene-specific DNA primers used to check their genotypes with PCR are shown in Table S2.

To overexpress *BRXL4*, a genomic fragment of *BRXL4* was amplified with an *Age*I site at the 5′ end and a *Bam*HI site at the 3′ end. A 2.5 kb of the BRXL4 promoter region was also amplified with *Sac*I site at the 5′ end and an *Age*I site at the 3′ end. These two amplified fragments were inserted between the *Sac*I/*Bam*HI sites of the binary vector pEGAD (Cutler et al., 2000) using GeneArt Seamless Cloning (www.thermofisher.com) to generate a native promoter overexpression construct. In addition, the *BRXL4* fragment was inserted between the *Age*I/*Bam*HI sites of pEGAD to generate a 35S-driven overexpression construct. The *Sac*I/*Age*I sites of pEGAD were used to insert the *BRXL4* promoter fragment to generate pBRXL4-eGFP-NLS. The SV40 NLS was inserted in the *Eco*RI and *Bam*HI sites after the eGFP. Arabidopsis plants were transformed using the floral dip method (Clough & Bent, 1998).

Phenotype measurements

To measure inflorescence branch angles, seedlings were first grown for 10–14 days on agar plates under continuous light in an incubator and then transplanted to soil and grown for 3–5 weeks in a growth chamber maintained at 22°C and illuminated with approximately 90 μmol m^{-2} sec^{-1} of white light on a 16 h light/8 h dark cycle. Inflorescences were harvested and trimmed to produce a 4-cm section containing the most basal node and 2 cm of its branch. Digital images of these sections were collected with a flatbed scanner, and the branch angle measured as previously described (Yoshihara et al., 2013).

Etiolated hypocotyl gravitropism was measured as previously described (Yoshihara et al., 2013), except seedlings used in this study grew for 3 days rather than 2 days and the tip angle was measured manually from the digital images. Gravitropism of excised and trimmed primary inflorescence stems was also measured using infrared light and computer-controlled cameras as described (Yoshihara & Spalding, 2020), except that instead of manually measuring the angle of the tip at each 10-min time point, an image analysis algorithm was developed in the MATLAB computer programming language to automate the measurement. The analysis algorithm determined the midline of each stem present in each frame of an experimental time series even if one crossed another during the bending response. A straight line was fit to the most apical portion of the midline. Its angle relative to the horizon was recorded as the tip angle for that frame and plotted versus time.

Effect of BRXL4 on LAZY1 levels and subcellular redistribution

We used a temperature-inducible *pHSP18.2:AtLAZY1-eGFP* reporter gene (Yoshihara et al., 2013) to determine the effect of a *brxl4* mutation on the subcellular distribution of LAZY1. Etiolated 3-day-old wild type or *brxl4-1* seedlings growing on agar were placed in an incubator maintained at 37°C for 5 h to induce expression of the tagged LAZY1. GFP fluorescence was examined using a Zeiss 710 confocal microscope fitted with a C-Apochromat 40× water immersion lens. Laser (488 nm) intensity, pinhole size, and detector gain were the same for all trials. A trial consisted of one field of view collected from one hypocotyl. A custom image analysis procedure written in the MATLAB computer programming language quantified the GFP signal (500–560 nm) at the plasma membrane. A Gaussian filter (21 × 21 pixels, SD = 4) applied to the 12-bit GFP channel increased the signal to noise ratio. The Otsu threshold value (Otsu, 1979) was used to create a binary mask, the mask was skeletonized, and then recursively de-spurred to produce a single pixel-wide representation of the plasma membranes in the captured focal plane. Branch points were removed to produce segments of plasma membrane. The longest segments (top quintile for length) were subjected to a three-pixel dilation. The intensity values of the pixels within these segments were averaged to measure the amount of LAZY1-GFP at the plasma membranes. To sample nuclear LAZY1-GFP, a human clicked on each visible nucleus to create a circular sample patch with a radius of seven pixels. The average GFP channel value within this patch was recorded.

Measuring mRNA by reverse transcription-qPCR

The GeneJET Plant RNA Purification Kit (www.thermofisher.com) was used to extract total RNA from either 3 days-old etiolated seedlings or 4-week-old inflorescence stems. Treatment with TURBO DNase (www.thermofisher.com) removed genomic DNA from the RNA extracts. Reverse transcription-quantitative (q) PCR was conducted using Luna Universal One-Step reverse transcription-qPCR Kit (www.neb.com) and a Mx3000P QPCR system (www.agilent.com) with the comparative $\Delta\Delta C_T$ method (Livak & Schmittgen, 2001). Equal amounts of RNA (1500 ng) were used in the qPCR reactions. Arabidopsis UBQ10 mRNA served as the reference gene. The gene-specific primers used are listed in Table S2. Three biological replicates per genotype, including the wild type, and tissue type were performed. Three technical replicates of each sample were performed. The results of the technical replicates per sample were highly similar and were averaged to produce a single value per sample. That value was divided by the wild-type value for that gene (*BRXL4* or *LAZY1*) for that tissue (hypocotyl or inflorescence stem). These normalized values are plotted in Figure 6.

CONFLICT OF INTEREST

The authors declare no conflict of interest.

DATA AVAILABILITY STATEMENT

The figures display all the data that this study used to reach its conclusions. The corresponding author (spalding@wisc.edu) will provide the values displayed in the plots upon request.

SUPPORTING INFORMATION

Additional Supporting Information may be found in the online version of this article.

Movie S1. Representative gravitropic responses of inflorescence stems, recorded in dim red light using infrared illumination, in *brxl4-1*, *proBRXL4* overexpressor, and the wild type.
Movie S2. Representative gravitropic responses of etiolated hypocotyls, recorded in total darkness using infrared illumination, in *brxl4-1*, *proBRXL4* overexpressor, and the wild type.

Table S1. Genes isolated more than once in the Y2H screen for LAZY1 interactors.

Table S2. Primers used to determine the genotype of T-DNA mutants and to measure mRNA levels by quantitative RT-PCR.

Figure S1. Control experiments show that the n-terminal portion of YFP attached to either LAZY1 or BRXL4 does not interact with the c-terminus of YFP to create a functional fluorescent YFP protein. Left panels would show fluorescence corresponding to the cells in the right panel if the fluorescence complementation shown in Figure 1(b) was not due to BRXL4-LAZY1 interaction. Scale bar = 20 μm

Figure S2. Additional examples of the *brxl4* mutants and the *pro35S:BRXL4* overexpressor.

Figure S3. Basic–hydrophobic (BH) score profiles for LAZY1 and BRXL4 proteins. Peaks above the horizontal dashed line indicate locations of predicted BH domains that can associate proteins with membranes. The relationships between the predicted BH domains and the recognized domains of LAZY1 and BRXL4 are shown in Figure 2. The plot was generated with the software described in Brzeska et al. (1) and available as a Web service here: https://hpcwebapps.cit.nih.gov/bhsearch/.

Figure S4. BRXL4 overexpression affects LAZY1 subcellular distribution in etiolated hypocotyls. (a) LAZY1-GFP controlled by a heat shock promoter in a *lazy1* mutant is evident at the plasma membrane and nucleus. (b) In the *brxl4-1* mutant, LAZY1-GFP is less apparent in the nucleus and more apparent at the plasma membrane. The results in (a) and (b) are separate from the trials shown in Figure 7. They are presented for comparison with four examples of LAZY1-GFP in a *pro35S* BRXL4 overexpressor line shown in (c). BRXL4 overexpression caused LAZY1 to produce bright spots in the nucleus, and accumulate in the cytoplasm, making it difficult to distinguish from plasma membrane localization. Scale bars = 20 μm.

REFERENCES

Barbosa, I.C.R., Shikata, H., Zourelidou, M., Heilmann, M., Heilmann, I. & Schwechheimer, C. (2016) Phospholipid composition and a polybasic motif determine D6 PROTEIN KINASE polar association with the plasma membrane and tropic responses. *Development*, **143**, 4687–4700.

Beuchat, J., Li, S., Ragni, L., Shindo, C., Kohn, M.H. & Hardtke, C.S. (2010) A hyperactive quantitative trait locus allele of Arabidopsis BRX contributes to natural variation in root growth vigor. *Proceedings of the National Academy of Sciences of the United States of America*, **107**, 8475–8480.

Briggs, G.C., Mouchel, C.F. & Hardtke, C.S. (2006) Characterization of the plant-specific *BREVIS RADIX* gene family reveals limited genetic redundancy despite high sequence conservation. *Plant Physiology*, **140**, 1306–1316.

Brzeska, H., Guag, J., Remmert, K., Chacko, S. & Korn, E.D. (2010) An experimentally based computer search identifies unstructured membrane-binding sites in proteins: application to class I myosins, PAKS, and CARMIL. *Journal of Biological Chemistry*, **285**, 5738–5747.

Chang, C.-W., Couñago, R.L.M., Williams, S.J., Bodén, M. & Kobe, B. (2012) Crystal structure of rice importin-α and structural basis of its interaction with plant-specific nuclear localization signals. *The Plant Cell*, **24**, 5074–5088.

Clough, S.J. & Bent, A.F. (1998) Floral dip: a simplified method for Arobacterium-mediated transformation of *Arabidopsis thaliana*. *The Plant Journal*, **16**, 735–743.

Cutler, S.R., Ehrhardt, D.W., Griffitts, J.S. & Somerville, C.R. (2000) Random GFP::cDNA fusions enable visualization of subcellular structures in cells of Arabidopsis at a high frequency. *Proceedings of the National Academy of Sciences of the United States of America*, **97**, 3718–3723.

Dardick, C.D., Scorza, R. & Hollender, C.A. (2017) Genetically altered plants having weeping phenotype. United States Patent Application. 20190062381.

Dong, Z., Jiang, C., Chen, X., Zhang, T., Ding, L., Song, W. *et al.* (2013) Maize LAZY1 mediates shoot gravitropism and inflorescence development through regulating auxin transport, auxin signaling, and light response. *Plant Physiology*, **163**, 1306–1322.

Furutani, M., Hirano, Y., Nishimura, T., Nakamura, M., Taniguchi, M., Suzuki, K. *et al.* (2020) Polar recruitment of RLD by LAZY1-like protein during gravity signaling in root branch angle control. *Nature Communications*, **11**, 76.

Godbole, R., Takahashi, H. & Hertel, R. (1999) The *lazy* mutation in rice affects a step between statoliths and gravity-induced lateral auxin transport. *Plant Biology*, **1**, 379–381.

Gookin, T.E. & Assmann, S.M. (2014) Significant reduction of BiFC non-specific assembly facilitates in planta assessment of heterotrimeric G-protein interactors. *The Plant Journal*, **80**, 553–567.

Hollender, C.A., Hill, J.L., Waite, J. & Dardick, C. (2020) Opposing influences of *TAC1* and *LAZY1* on lateral shoot orientation in Arabidopsis. *Scientific Reports*, **10**, 6051.

Howard, T.P., III, Hayward, A.P., Tordillos, A., Fragoso, C., Moreno, M.A., Tohme, J. *et al.* (2014) Identification of the maize gravitropism gene *lazy plant1* by a transposon-tagging genome resequencing strategy. *PLoS One*, **9**, e87053.

Jiao, Z., Du, H., Chen, S., Huang, W. & Ge, L. (2021) *LAZY* gene family in plant gravitropism. *Frontiers in Plant Science*, **11**, 606241.

Jones, J.W. & Adair, C.R. (1938) A "lazy" mutation in rice. *Journal of Heredity*, **29**, 315–318.

Kagale, S. & Rozwadowski, K. (2011) EAR motif-mediated transcriptional repression in plants. *Epigenetics*, **6**, 141–146.

Kleine-Vehn, J., Ding, Z., Jones, A.R., Tasaka, M., Morita, M.T. & Friml, J. (2010) Gravity-induced PIN transcytosis for polarization of auxin fluxes in gravity-sensing root cells. *Proceedings of the National Academy of Sciences of the United States of America*, **107**, 22344–22349.

Koh, S.W.H., Marhava, P., Rana, S., Graf, A., Moret, B., Bassukas, A.E.L. *et al.* (2021) Mapping and engineering of auxin-induced plasma membrane dissociation in BRX family proteins. *The Plant Cell*, **33**, 1945–1960.

Li, P., Wang, Y., Qian, Q., Fu, Z., Wang, M., Zeng, D. *et al.* (2007) LAZY1 controls rice shoot gravitropism through regulating polar auxin transport. *Cell Research*, **17**, 402–410.

Li, Z., Liang, Y., Yuan, Y., Wang, L., Meng, X., Xiong, G. *et al.* (2019) *OsBRXL4* regulates shoot gravitropism and rice tiller angle through affecting LAZY1 nuclear localization. *Molecular Plant*, **12**, 1143–1156.

Livak, K.J. & Schmittgen, T.D. (2001) Analysis of relative gene expression data using real-time quantitative PCR and the $2^{-\Delta\Delta CT}$ method. *Methods*, **25**, 402–408.

Marhava, P., Aliaga Fandino, A.C., Koh, S.W.H., Jelínková, A., Kolb, M., Janacek, D.P. *et al.* (2020) Plasma membrane domain patterning and self-reinforcing polarity in Arabidopsis. *Developmental Cell*, **52**, 223–235.e225.

Marhava, P., Bassukas, A.E.L., Zourelidou, M., Kolb, M., Moret, B., Fastner, A. *et al.* (2018) A molecular rheostat adjusts auxin flux to promote root protophloem differentiation. *Nature*, **558**, 297–300.

Morita, M.T. (2010) Directional gravity sensing in gravitropism. *Annual Review of Plant Biology*, **61**, 705–720.

Mouchel, C.F., Briggs, G.C. & Hardtke, C.S. (2004) Natural genetic variation in Arabidopsis identifies BREVIS RADIX, a novel regulator of cell proliferation and elongation in the root. *Genes & Development*, **18**, 700–714.

Nakamura, M., Nishimura, T. & Morita, M.T. (2019) Bridging the gap between amyloplasts and directional auxin transport in plant gravitropism. *Current Opinion in Plant Biology*, **52**, 54–60.

Otsu, N. (1979) A threshold selection method from gray-level histograms. *IEEE Transactions on Systems, Man, and Cybernetics*, **9**, 62–66.

Overbeek, J.V. (1938) "Laziness" in maize due to abnormal distribution of growth hormone. *Journal of Heredity*, **29**, 339–341.

Reuter, L., Schmidt, T., Manishankar, P., Throm, C., Keicher, J., Bock, A. *et al.* (2021) Light-triggered and phosphorylation-dependent 14-3-3 association with NON-PHOTOTROPIC HYPOCOTYL 3 is required for hypocotyl phototropism. *Nature Communications*, **12**, 6128.

Roychoudhry, S., Kieffer, M., Del Bianco, M., Liao, C.-Y., Weijers, D. & Kepinski, S. (2017) The developmental and environmental regulation of gravitropic setpoint angle in Arabidopsis and bean. *Scientific Reports*, **7**, 42664.

Scacchi, E., Osmont, K.S., Beuchat, J., Salinas, P., Navarrete-Gómez, M., Trigueros, M. *et al.* (2009) Dynamic, auxin-responsive plasma membrane-to-nucleus movement of Arabidopsis BRX. *Development*, **136**, 2059–2067.

Smith, H.M.S. & Raikhel, N.V. (1999) Protein targeting to the nuclear pore. What can we learn from plants? *Plant Physiology*, **119**, 1157–1164.

Spalding, E.P. (2013) Diverting the downhill flow of auxin to steer growth during tropisms. *American Journal of Botany*, **100**, 203–214.

Su, S.-H., Gibbs, N.M., Jancewicz, A.L. & Masson, P.H. (2017) Molecular mechanisms of root gravitropism. *Current Biology*, **27**, R964–R972.

Taniguchi, M., Furutani, M., Nishimura, T., Nakamura, M., Fushita, T., Iijima, K. *et al.* (2017) The Arabidopsis LAZY1 family plays a key role in gravity signaling within statocytes and in branch angle control of roots and shoots. *The Plant Cell*, **29**, 1984–1999.

van Overbeek, J. (1936) "Lazy," an a-geotropic form of maize:"gravitational response" rather than structural weakness accounts for prostrate growth-habit of this form. *Journal of Heredity*, **27**, 93–96.

Waite, J.M. & Dardick, C. (2018) *TILLER ANGLE CONTROL 1* modulates plant architecture in response to photosynthetic signals. *Journal of Experimental Botany*, **69**, 4935–4944.

Waite, J.M. & Dardick, C. (2021) The roles of the IGT gene family in plant architecture: past, present, and future. *Current Opinion in Plant Biology*, **59**, 101983.

Wang, W., Gao, H., Liang, Y., Li, J. & Wang, Y. (2021) Molecular basis underlying rice tiller angle: current progress and future perspectives. *Molecular Plant*, **15**, 125–137.

Wender, N.J., Polisetty, C.R. & Donohue, K. (2005) Density-dependent processes influencing the evolutionary dynamics of dispersal: a functional analysis of seed dispersal in *Arabidopsis thaliana* (Brassicaceae). *American Journal of Botany*, **92**, 960–971.

Yang, J., Liu, Y., Yan, H., Tian, T., You, Q., Zhang, L. *et al.* (2018) PlantEAR: functional analysis platform for plant EAR motif-containing proteins. *Frontiers in Genetics*, **9**, 590.

Ye, C.-Y., Tang, W., Wu, D., Jia, L., Qiu, J., Chen, M. *et al.* (2019) Genomic evidence of human selection on Vavilovian mimicry. *Nature Ecology & Evolution*, **3**, 1474–1482.

Yoshihara, T. & Iino, M. (2007) Identification of the gravitropism-related rice gene LAZY1 and elucidation of LAZY1-dependent and -independent gravity signaling pathways. *Plant & Cell Physiology*, **48**, 678–688.

Yoshihara, T. & Spalding, E.P. (2017) LAZY genes mediate the effects of gravity on auxin gradients and plant architecture. *Plant Physiology*, **175**, 959–969.

Yoshihara, T. & Spalding, E.P. (2020) Switching the direction of stem gravitropism by altering two amino acids in AtLAZY1. *Plant Physiology*, **182**, 1039–1051.

Yoshihara, T., Spalding, E.P. & Iino, M. (2013) AtLAZY1 is a signaling component required for gravitropism of the *Arabidopsis thaliana* inflorescence. *The Plant Journal*, **74**, 267–279.